HHS Public Access

Author manuscript

Phytochemistry. Author manuscript; available in PMC 2017 February 01.

Published in final edited form as:

Phytochemistry. 2016 February ; 122: 11–21. doi:10.1016/j.phytochem.2015.11.002.

Characterization of an epoxide hydrolase from the Florida Red tide dinoflagellate, *Karenia brevis*

Pengfei Sun[a], **Cristian Leeson**[a], **Xiaoduo Zhi**[a], **Fenfei Leng**[a], **Richard H. Pierce**[b], **Michael S. Henry**[b], and **Kathleen S. Rein**[a,*]

Pengfei Sun: psun001@fiu.edu; Fenfei Leng: lengf@fiu.edu; Richard H. Pierce: rich@mote.org; Michael S. Henry: mhenry@mote.org

[a]Department of Chemistry and Biochemistry, Florida International University, Miami, FL 33199

[b]Mote Marine Laboratory, 1600 Ken Thompson Parkway, Sarasota, FL 34236, USA

Abstract

Epoxide hydrolases (EH, EC 3.3.2.3) have been proposed to be key enzymes in the biosynthesis of polyether (PE) ladder compounds such as the brevetoxins which are produced by the dinoflagellate *Karenia brevis*. These enzymes have the potential to catalyze kinetically disfavored *endo-tet* cyclization reactions. Data mining of *K. brevis* transcriptome libraries revealed two classes of epoxide hydrolases: microsomal and leukotriene A_4 (LTA_4) hydrolases. A microsomal EH was cloned and expressed for characterization. The enzyme is a monomeric protein with molecular weight 44 kDa. Kinetic parameters were evaluated using a variety of epoxide substrates to assess substrate selectivity and enantioselectivity, as well as its potential to catalyze the critical *endo-tet* cyclization of epoxy alcohols. Monitoring of EH activity in high and low toxin producing cultures of *K. brevis* over a three week period showed consistently higher activity in the high toxin producing culture implicating the involvement of one or more EH in brevetoxin biosynthesis.

Graphical Abstract

Epoxide hydrolases are believed to be key enzymes in the biosynthesis of brevetoxins. Significant differences in epoxide hydrolase activity and expression in high and low toxin strains of *Karenia brevis* support this hypothesis.

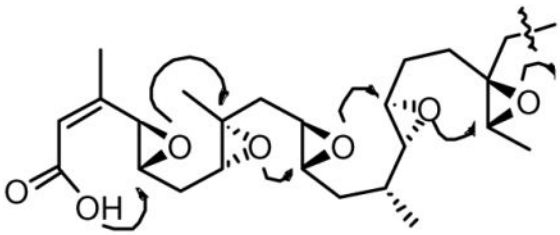

Kathleen Rein: reink@fiu.edu, 11200 SW 8th St., Miami. FL 33199, Phone: 305-348-6682, FAX: 305 348-3772.

Keywords

dinoflagellate; *Karenia brevis*; *Prorocentrum hoffmanianum*; Dinophyceae; protein biochemistry; brevetoxin; epoxide hydrolase

1. Introduction

The brevetoxins (e.g. brevetoxin B (**1**)) (Scheme 1) are produced by *Karenia brevis*, the principal HAB organism in the Gulf of Mexico also known as the Florida red tide dinoflagellate. These polyether ladder compounds are responsible for massive fish kills, marine mammal mortalities and, in humans, neurotoxic shellfish poisoning (NSP) and asthma-like symptoms through ingestion or inhalation exposures, respectively (Fleming et al., 2005; Flewelling et al., 2005; Van Dolah et al., 2003). The brevetoxins are representative of a larger group of marine algal toxins known as polyether (PE) ladders which includes ciguatoxins and yessotoxins. These molecules share common structural features which include a series of *trans*-fused polyether rings with oxygen atoms alternating across the "top" and "bottom" of the molecules. Shortly after their structures were determined in the 1980's, efforts to understand the biosynthesis of these complex molecules began. Stable isotope incorporation experiments using ^{13}C-labelled acetate established the polyketide origins of the brevetoxins, yet some anomalies in the labeling patterns, were also observed (Chou and Shimizu, 1987; Lee et al., 1989; Lee et al., 1986). Since then, similar patterns have been observed in other PE ladder compounds (Bourdelais et al., 2005; Gallimore and Spencer, 2006). As a class of compounds, polyketides are structurally diverse yet share a common biogenic pathway which is highly analogous to fatty acid biosynthesis. The carbon skeletons are constructed by the sequential condensation of small carboxylic acid subunits in a series of reactions catalyzed by a polyketide synthase (PKS). While transcripts coding for functional domains of PKSs including ketosynthases (KS), ketoreductase (KR), and an acyl carrier proteins (ACP) have been identified, *K. brevis* appears to have a PKS architecture which is distinct from those of bacteria, plants or fungi (Monroe and Van Dolah, 2008; Snyder et al., 2003; Snyder et al., 2005).

While the origins of the carbon atoms in the brevetoxins have been determined, the remainder of the polyether ladder pathway has yet to be determined. The prevailing hypothesis, put forth nearly 30 years ago by Nakanishi, suggests that PKS-mediated synthesis of the polyene is followed by epoxidation to afford a polyepoxide which then undergoes an epoxide-opening cascade, catalyzed by an epoxide hydrolase (EH), to provide the polyether (brevetoxin B, **1** in the example shown in Scheme 1) (Lee et al., 1989; Nakanishi, 1985). This hypothesis, which remains unconfirmed, accounts for the oxygen-carbon-carbon (O–C–C) connectivity pattern and *trans-syn* topography in the natural products and is supported by the recent identification of molecular oxygen (O_2) as the source of the ether oxygen atoms in the structurally similar PE ladder yessotoxin, produced by the dinoflagellate *Protoceratium reticulatum* (Yamazaki et al., 2012).

The scheme proposed by Nakanishi for brevetoxin biosynthesis is conceptually analogous to the biosynthesis of monensin (**2**) and other bacterial, non-ladder (linked) polyethers, wherein an EH is the key enzyme responsible for the construction of the polyether rings (Gallimore

and Spencer, 2006; Matsuura et al., 2010; Minami et al., 2011; Shichijo et al., 2008). An alternative proposal for PE ladder biosynthesis suggests that chain extension, epoxidation and cyclization may be performed in an iterative process (Gallimore and Spencer, 2006). At this time, no gene or enzyme has been definitively linked to polyketide biosynthesis in a dinoflagellate. This is in part due to the size and complexity of the dinoflagellate genome, and the lack of a transformation system.

In the work reported herein, a study was carried out to identify and characterize one or more epoxide hydrolases from *K. brevis* and to investigate their potential role in brevetoxin biosynthesis.

2. Results and Discussion

2.1 Epoxide hydrolase activity in cell free extracts

Efforts to identify and characterize epoxide hydrolases from *K. brevis* began by examining a cell free extract (CFE) using a sensitive fluorescent assay. Substrate (**5a**) (see Scheme 2) was prepared from *trans*-styrylacetic acid and 7-methoxy-2-napthaldehyde, **4** as previously described (Jones, et al, 2005). Typically, an epoxide hydrolase will catalyze epoxide ring opening to yield the corresponding 1,2-diol. An EH catalyzed hydrolysis of the epoxide substrate, **5a** produces an intermediate diol which lactonizes to release the fluorescent reporter **4** (Scheme 2) after hydrolysis of the intermediate cyanohydrin. It was reasoned that a substrate containing aliphatic rather than aromatic substituents would be more representative of the native substrate if it were involved in brevetoxin biosynthesis. Thus a second probe (**5b**) was prepared from *trans*-3-hexenoic acid according to the procedure described for the synthesis of **5a** (Jones, et al, 2005). Activity was detected in *K. brevis* CFE using both probes, but probe **5b** proved to be the better substrate as anticipated (Figure 1A). The ratio of initial rates (V_o) for substrates **5a:5b** was 1:3. In CFE, probes **5a** and **5b** will detect both EH and esterase activity. However, the alkene precursors can be used to assess for esterase activity alone. Higher levels of activity were observed when using the epoxide probes **5a/b** when compared to the alkene probes **3a/3b,** giving rise to the possibility that both esterase and EH activity were being detected by the epoxide probes. Therefore, all assays of CFE were corrected for esterase activity by subtracting the absorbance values obtained with the corresponding esterase probes. The ratios of initial rates were comparable (2.02, σ= 0.17, n = 5 and 2.16, σ = 0.19, n = 8: represents average of n experiments, each experiment performed in duplicate or triplicate) for the **5a/3a** and **5b/3b** pairs when assayed under identical conditions. Finally, the EH and esterase activities of CFE were evaluated from the dinoflagellate *Prorocentrum hoffmanianum*, producer of the linear polyether okadaic acid **6** (Figure 2) which consists of only two fused ether rings. Because the proposed biosynthesis of okadaic acid **6** would involve a single epoxide ring opening reaction, it is interesting and perhaps noteworthy that the initial rates of EH activity (normalized to protein) for *K. brevis* CFE was more than two-fold greater than that of *P. hoffmanianum* CFE (2.3:1). Furthermore, in *P. hoffmanianum*, esterase activity was higher than EH activity (Figure 1D).

Three types of EH, which operate through distinct catalytic mechanisms, have been identified (Morisseau and Hammock, 2005). The most studied of these belong to the larger

family of hydrolases containing an α,β-fold and are often referred to as α,β-hydrolases. Two conserved tyrosine residues and a conserved Asp-His-Asp catalytic triad make up the active site. The tyrosines are believed to serve as general acids for activation of the epoxide by forming two hydrogen bonds with the oxygen (Yamada et al., 2000). The carboxylate group of one of the Asp residues is activated by the His and second Asp in the active site and is the nucleophile that attacks the epoxide, typically at the least substituted carbon. In a second step, a water molecule, activated by the His-Asp charge relay, cleaves the ester that is formed, liberating the diol and regenerating the enzyme (Scheme 3A). A second type of EH is the leukotriene-A_4 (LTA_4) hydrolase (Rudberg et al., 2004). The LTA_4 hydrolase is highly substrate specific, converting LTA_4 into leukotriene-B_4 (LTB_4). Only two other substrates, the double bond isomers LTA_3 and LTA_5, have been identified for this EH. In this enzyme active site, two histidines and a glutamate coordinate a Zn^{2+} ion, which in turn coordinates the epoxide oxygen. Upon activation of the 5, 6-epoxide, an intermediate carbocation, whose charge is delocalized over a conjugated triene system, is quenched at C-12 by a water molecule which is activated and delivered by a conserved Asp residue, to produce a 5, 12-diol rather than a 1, 2-diol (Scheme 3B). A covalent adduct between the enzyme and substrate is not formed in this process making it distinct from the α,β-hydrolase type. The third EH is the limonene-1,2-epoxide hydrolase (LEH). In this case, the epoxide is activated by hydrogen bonds to an Asp residue. However, as in the case of LTA_4 hydrolase, a water molecule is activated and delivered by Asn, Asp and Tyr residues in a one-step mechanism and a covalent intermediate is not formed (Arand et al., 2003). EHs which are involved in the biosynthesis of non-ladder type polyethers are of the LEH type. Genes coding for LEHs have been identified in the biosynthetic gene clusters for the bacterial polyethers monenesin (**2**) (Oliynyk et al., 2003), lasalocid (Smith et al., 2008), nanchangmycin (Sun et al., 2003), tetronomycin (Demydchuk et al., 2008) and nigericin (Harvey et al., 2007). In the case of monensin (**2**) and lasalocid, EH encoding genes have been expressed and the EH activity of the enzymes confirmed (Minami et al., 2011; Minami et al., 2013).

The EH activity of *K. brevis* CFE was examined in the presence of known inhibitors of two of the three classes of EH: adamantly urea **7**, inhibitor of mouse (K_i of 0.33 μM) and human (K_i of 6.2 μM) α,β-hydrolase type (Kim et al., 2004) and inhibitors of the *Rhodococcus erythropolis* LEH: valpromide **8** (K_i of 100 μM) (Arand et al., 2003). Due to the substrate specificity and unique mechanism of the LTA_4 hydrolase, it is unlikely that our probes would detect such activity. Among the two EH inhibitors tested, only adamantly urea **7** inhibited the total activity in the *K. brevis* CFE (Figure 1B) when using probe **5a** as the substrate. At equal concentrations (100 μM) of substrate **5a** and inhibitor, a 44% inhibition was observed in the presence of adamantyl urea **7**. Esterase activity was not inhibited by either of the two EH inhibitors. These data suggest that the observed EH activity in *K. brevis* CFE can be attributed to an epoxide hydrolases of the α,β-hydrolase type.

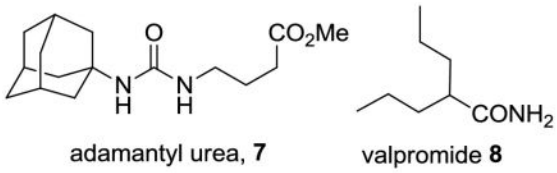

2.2 Identification, cloning and expression of an EH from *K. brevis*

tBLASTn (Altschul et al., 1990) analysis of a *K. brevis* EST library consisting of 22,000 predicted transcripts (Lidie et al., 2005) against *Rhodococcus erythropolis* LEH and nine other known or putative LEHs which are associated with biosynthetic gene clusters of bacterial polyethers: monenesin (**2**) (MonB1 and MonB2), lasalocid (Lsd19A and Lsd19B), nanchangmycin (NanIA and NanIB), tetronomycin (TmnB), nigericin (NigB1 and NigB3) was performed. All failed to return any significant homologies with the smallest Expect values on the order of 10^{-5} tBLASTn analysis against *Emeliania huxleii* LTA_4 hydrolase (NCBI Accession number: XP_005787867) returned a single transcript having an Expect value smaller than 10^{-5} (3×10^{-6}). However, BLASTx analysis of the single transcript did not return significant homologies to any other LTA_4 hydrolase. tBLASTn analysis of the *K. brevis* EST library against a variety of prokaryotic and eukaryotic EHs of the α, β-hydrolase type revealed a transcript (MGID2034061) with significant homologies having Expect values ranging from 10^{-126} to 10^{-103}. The identified EST coded for a 393 amino acid protein (EH1) with a calculated molecular weight of 44.6 kDa. BLASTp analysis of this protein against the NCBI non-redundant protein database returned a putative hydrolase with Expect value of 10^{-126}, from the polar, eukaryotic microalga *Coccomyxa subellipsoidea* (Blanc et al., 2012) as the closest match. Figure 3A shows the alignment of the translated protein with theα, β-hydrolase type EH from *Aspergillus niger* (NCBI Accession Number: CAB 49813.1;(Zou et al., 2000)). The two conserved catalytic tyrosine residues can be identified in the translated protein. However, the Asp-His-Asp catalytic triad is replaced with Asp-His-Glu. After optimization of the codon usage for *E. coli* expression, the putative *K. brevis* EH gene was synthesized, cloned into pUC 57 and subcloned into pET30a+ for expression with the incorporation of six C-terminal histidine codons to facilitate purification of the expressed protein. As shown in Figure 3B, the purified protein has the anticipated molecular weight of 44 kDa.

2.3 Characterization of *K. brevis* EH

Fluorescent probe sets **3b**/**5b** and **3a**/**5a** were used for initial characterization of the expressed *K. brevis* EH (Figure 3C). The EH was optimally active at pH 6.8 ~7.1, with half-maximal activity at pH 6.5 and 8.3. Consistent with the selectivity observed in the *K. brevis* CFE, the purified EH showed a preference for epoxide **5b** over **5a**. The ratio of initial rates (V_o) for substrates **5a:5b** was 1:4. Epoxide hydrolases of the α,β-hydrolase type share significant homologies with other hydrolases, including esterases. As done with the CFE, EH activity was distinguished from esterase activity using the substrates **3a** and **5a**. No activity was observed using the esterase probes indicating that the expressed protein was indeed an EH.

Substrate and enantioselectivity of the *K. brevis* EH was assessed by kinetic studies. Kinetic parameters of the enzyme using substrates **5a** and **5b** were performed using the sensitive fluorescent assay. Other substrates having no fluorescent reporter group were evaluated by GC-MS analysis of the reaction mixtures using 1-naphthol as an internal standard. The data shown in Table 1 indicates that the *K. brevis* EH has a strong preference for terminal epoxides over internal epoxides (Entries 3–9 vs. Entries 1–2). Aliphatic substituents are preferred over aromatic substituents by approximately 5:1 (Entries 7–9 vs. Entries 3–6) and the enzyme shows only a slight preference for *R* over *S* enantiomers (Entries 3 and 4). The reaction rates using 1,2-disubstituted epoxides as substrates are too slow to be determined using the GC-MS method. However, disubstituted epoxides proved to be inhibitors of the *K. brevis* EH only when an aromatic substituent is present (Entries 10–12 vs. Entries 13–14) and *cis*-disubstituted epoxides are more potent inhibitors than those that are *trans*-disubstituted (Entries 10–12).

A noteworthy distinction between the monensin (**2**) pathway and the proposed brevetoxin (**1**) pathway is the site of nucleophilic attack on the epoxide substrate (Scheme 1). In the case of non-ladder polyethers, the majority of epoxide ring opening reactions proceed via attack at the proximal carbon (*exo-tet* cyclization) while polyether ladder formation requires attack at the distal carbon (*endo-tet* cyclization). Both the empirical Baldwin's rules (Baldwin, 1976) and molecular orbital calculations (Gruber et al., 1999) indicate that the *endo-tet* cyclization pathway is kinetically disfavored. The exception among the bacterial polyketides is lasalocid. In this polyether, the pyran ring arises from the *endo-tet* cyclization of an intermediate epoxide. This reaction is catalyzed by the EH Lsd19. Lsd19 is a bifunctional enzyme consisting of two domains (A and B). Each domain is responsible for the cyclization of one of the rings with Lsd19B catalyzing the *endo-tet* cyclization of the terminal ring (Minami et al., 2011).

The ability of the *K. brevis* EH to perform cyclization was also evaluated. The substrate *trans*-4,5-epoxy-hexanol **9** was prepared as previously described (Coxon et al., 1973). This substrate may undergo *endo-tet* cyclization to produce pyran **10**, or *exo-tet* cyclization to produce furan **11** (Scheme 4). The substrate was incubated with the expressed EH in reaction buffer and the reaction was monitored by GC-MS. Both possible products were identified by GC-MS, by comparison with authentic samples however, neither the percent conversion nor the product ratio differed from that of the buffer alone.

2.4 EH activity/expression and toxin content over the life of a culture

Two cultures of *K. brevis* whose toxin content differs by ten-fold were evaluated over a period of three weeks for EH activity and EH mRNA levels. Both cultures are of the Wilson strain. However, toxin production of one culture dropped significantly for reasons which are not understood. Cellular brevetoxin (**1**) content in both cultures was determined by LC-MS with the higher toxin culture having 5–6.8 pg/cell, whereas the low toxin culture had only 0.002–0.05 pg/cell. EH activity was assessed using the EH/esterase probe set **3b**/**5b**. Esterase activity, determined using probe **3b**, was subtracted from total activity, determined using probe **5b**. Cultures were diluted on day 0 to equal cell counts and monitored over a 21 day period. As shown in Figure 4A, EH activity for the high toxin culture was consistently

higher than that of the low toxin culture. On average, EH activity for the high toxin culture was 18% and 60% higher than the low-toxin culture when normalized to protein content or to cell counts, respectively. A two tailed *t*-test confirms that there is a significance difference in EH activity when normalized to protein ($p = 8 \times 10^{-14}$) or normalized to cell counts ($p = 2 \times 10^{-6}$). Over the three weeks that the cultures were monitored, both showed a slight drop in EH activity when normalized to protein content and an increase in activity when normalized to cell counts. Expression of the EH mRNA was also monitored over the same period by Q-PCR. Figure 4B shows the ratio of cycle thresholds (C_t) for the EH mRNA normalized to RuBisCO mRNA. EH mRNA levels of the low toxin culture were either lower (C_t higher) or equal to (day 19 only) that of the high toxin culture. Even though gene expression in dinoflagellates is believed to occur principally at the translational level (Greenbaum et al., 2003), a significant difference in the average ratio of C_t values was observed over the life of the culture ($p = 0.02$).

2.5 Additional library searches

Subsequent to these studies, three *K. brevis* reference transcriptome libraries containing 86,580 (Wilson strain), 93,668 (strain SP1) and 84,309 (strain SP3) predicted transcripts (Ryan et al., 2014) became available. tBLASTn analysis of these transcriptome libraries against the 10 LEHs and the *Emeliania huxleii* LTA_4 hydrolase were performed. Against the LEHs, a single transcript from the SP1 transcriptome returned an Expect values of less than 10^{-5} (4×10^{-6}) against NanIB. However, BLASTx analysis against the NCBI non-redundant protein database did not return any significant homologies (10^{-6} or less). Against the *E. huxleii* LTA_4 hydrolase, numerous transcripts with expect values ranging from 10^{-12} to10^{-141} were identified from all three libraries.

The cDNA sequence of the α,β-epoxide hydrolase (EH1) was used as a query for a nucleotide BLAST analysis of the three reference transcriptomes. Each of these transcriptome libraries returned sequences (EH2) which were identical to each other (Locus 28231 from SP1; Locus 35217 from SP3; Locus 51025 from Wilson) having Expect values ranging from 10^{-79} to10^{-84}. Additionally, a single transcript, which was identical to the query sequence, was identified in the SP3 library (SP3 Locus 73930). When the newly identified sequence (EH2, Locus 28231 from SP1) was used as a query to search the original EST library, a single 50 bp sequence was returned which exactly matched the query. The alignment of these two α,β-epoxide hydrolases is shown in Figure 5. These two hydrolases share 35% identity and 57% similarity. α,β Epoxide hydrolases exhibit two active site variations: the identity and location of the charge relay acid which may be either Asp or Glu and may be located either after a central β-strand (β6) or after β7: and the presence or absence of the second Tyr (Barth et al., 2004). The two *K. brevis* EHs are similar in that each has two active site Tyrs as well as a Glu located after β7. Within the α,β fold epoxide hydrolases, there are three classes which may be broadly characterized by their highly variable N-terminal domains (Barth et al., 2004): the soluble (or cytosolic) EH (sEH): the microsomal EH (mEH) and the plant EHs which lack this N-terminal domain entirely. The mEHs are believed to be involved in the metabolism of xenobiotics whereas the sEHs are thought to be involved in metabolism of fatty acids (Morisseau and Hammock, 2005). However, only mammalian genomes encode both sEH and mEH, whereas yeast, fungi,

insects and plants encode only one type and the activity of the absent EH type may be assumed by the other. Both of the α,β fold type EHs identified in *K. brevis* belong to the mEH class (Barth et al., 2004; Pleiss et al., 2000). The N-terminal domains of mEHs are characterized by a microsomal domain which may or may not be preceded by an N-terminal membrane anchor. The membrane anchor is found in mammalian and insect mEHs, but not in EHs from yeast, fungi or bacteria and is also absent in the two *K. brevis* mEHs. EHs may be further categorized according to the length of two loops: the NC-loop which links the N-terminal catalytic domain and the cap domain (the cap domain contains the two catalytic Tyr) and the cap-loop, which links two α-helices (α6 and α7) within the cap domain (Barth et al., 2004). The length of these loops may be determined from the pair wise alignment with the EH from *A. niger* (also an mEH) or by inspection of a homology model constructed using the *A. niger* EH crystal structure as template (Arand et al., 1999). In *A. niger*, the NC loop is located from Leu215 to Leu249 (35 residues) whereas the cap-loop is located from Trp284 to Ser291 (8 residues). The lengths of the NC loops of the *K. brevis* EHs are 36 and 43 residues, whereas both cap-loops are 14 residues. mEHs are characterized by having long to very long NC-loops (33 or more residues) and short to medium cap-loops (8–36). The *K. brevis* NC-loops and cap-loops would be considered very long and medium in length, respectively. The length of these domains is believed to govern substrate selectivity of the EH and this combination of long/med NC-loop/cap-loop would suggest selectivity for aromatic epoxides. The *K. brevis* EH1 appears to deviate from this generalization as selectivity was observed for aliphatic over aromatic substituted epoxides. Like the *K. brevis* EH1, the mEH from *A. niger* is unable to catalyze the hydrolysis of non-terminal epoxides (Pedragosa-Moreau et al., 1996a). However, the mEH from *A. niger* has a more pronounced enantioselectivity with relative rates of hydrolysis of *R:S p*-nitrostyrene of 55:1 (Morisseau et al, 1999).

3. Concluding remarks

Data mining of four transcriptome libraries indicates that *K. brevis* expresses two of the three main classes of epoxide hydrolases: LTA_4 hydrolase and the α,β fold type of epoxide hydrolases. Representatives of the limonene type of epoxide hydrolase were not identified in these libraries which is consistent with inhibition assays performed on CFE. The involvement of limonene epoxide hydrolases in the biosynthesis of bacterial polyethers has been firmly established, and it has long been believed that the dinoflagellate derived polyether ladders share a common biogenic origin with bacterial polyethers including involvement of one or more epoxide hydrolases. Thus the absence of LEH comes as somewhat of a surprise. Given the high substrate specificity of the LTA_4 hydrolases, their involvement in polyether ladder biosynthesis seems unlikely. Two EHs of the α,β fold type were identified in the transcriptome libraries.

The selectivity of the expressed *K. brevis* EH for aliphatic epoxides coupled with the consistently higher level of EH activity in the high toxin vs low toxin cultures of *K. brevis* is intriguing and suggests the involvement of this EH in brevetoxin biosynthesis. The expressed EH did not catalyze the cyclization of an epoxy alcohol to either a furan or pyran. However, epoxy alcohol **9** may not sufficiently resemble the native substrate. Lsd19 was also not capable of catalyzing the cyclization of monoepoxy alcohol which was significantly

smaller than pre-lasalocid (Matsuura et al., 2010). A key difference between the LEH and the α,β fold type of EH is in the mechanism. The LEH delivers a nucleophile, either a water molecule, or in the case of the bacterial polyethers, an alcohol, whereas the α,β fold type EH initially forms a covalent adduct with the nucleophilic Asp residue, which must ultimately be cleaved. It is therefore somewhat difficult to rationalize the involvement of the α,β fold type EH in PE ladder biosynthesis. Vilotijevic demonstrated that non-enzymatic *endo* selective epoxide-opening cascade reactions were promoted in water when templated by a single tetrahydropyran ring (Vilotijevic and Jamison, 2007). A vicinal diol formed by the enzymatic hydrolysis of an epoxide precursor by an α,β fold type EH, followed by cyclization to the brevetoxin lactone ring, could provide the template for a water promoted epoxide-opening cascade. It has further been suggested that an epoxidase could catalyze both epoxidation and cyclization for PE ladder formation without need for EH involvement (Gallimore and Spencer, 2006).

4. Experimental

4.1 Culture methods

K. brevis culture (Wilson strains) were obtained from Mote Marine Laboratory (Sarasota, Florida) and maintained in L1-Si medium, with the exception that the NH 15 vitamin supplement (Gates and Wilson, 1960) replaced the L-1 supplement, in a growth chamber at ~20°C under 35 μmol.photons.m^{-2}.s^{-1}. Growth was monitored by counting a 1:10 dilution of culture in Z pak reagent using a Beckman Z-series Coulter Counter with aperture size between 10~30 μm according to the manufacturer's instructions.

4.2 HPLC-MS/MS analysis of brevetoxins

Brevetoxins were extracted from *K. brevis* culture using a previously described method (Pierce and Henry, 2008). Quantitative analysis of brevetoxins and conjugates were conducted using a TSQ Quantum Access/ESI/Accela UHPLC for LC-MS/MS. The LC system consisted of a Thermo Electron Accela UHPLC pumping system, coupled with the Accela Autosampler and Degasser. The analytical column of consisted of a Kinetex C-18, reversed phase, 2.6um particle size with dimensions of 100mm × 2.1mm (Phenomenex, Torrance, CA). Mass Spectrometry was obtained using a TSQ Quantum Access MS/MS system, calibrated with brevetoxin standards from Marbionic (Wilmington, NC).

4.3 Preparation of K. brevis homogenate

K. brevis culture (200 ml) was concentrated by centrifugation (5 min at 450 × *g*) and the supernatant discarded. The cells were resuspended in phosphate buffer (800 μl, 50 mM pH 7.0) and vortexed for 1 min. This suspension was centrifuged (14,000 × *g* for 10 min) and the pellet was discarded. Homogenates were analyzed for protein concentration and glucose-6-phosphate dehydrogenase activity as described below. Typical protein concentrations ranged from (0.25 to 0.5 mg/ml).

4.4 Bradford assay

Five concentrations of BSA (0 mg/ml, 1 mg/ml, 0.5 mg/ml, 0.25 mg/ml, 0.0625 mg/ml) in phosphate buffer (50 mM, pH 7.0) were prepared as standards. Commassie Protein Assay

Reagent (250 μl) was added to microplate wells and 20 μl of standard or unknown sample were added. Absorbance was measured at 595 nm (Synergy™ 2, Bioteck Instrument, Inc.) after incubation for 5 min at room temperature. Each protein solution was assayed in duplicate.

4.5 Glucose-6-phosphate dehydrogenase activity

In order to ensure activity of *K. brevis* cell free extract (150 μl) was mixed with assay buffer (50 μl, 31 mM phosphate buffer, 7.5 mM glucose-6-phophate, 2.5 mM NADP, 38 mM $MgCl_2$). Absorbance at 340 nm was determined (Synergy™ 2, Bioteck Instrument, Inc.) after incubation for 1 h at room temperature. Blank control and boiled homogenate were also tested; typical activity of homogenate was more than twice that of boiled homogenate.

4.6 Probe synthesis

The fluorescent probe **5a** was prepared as previously described (Jones et al., 2005). A second probe **5b** was prepared in a procedure identical to that of **5a** except that (*E*)-4-phenylbut-3-enoic acid was replaced with (*E*)-pent-2-enoic acid. Both alkene and epoxide were purified by radial chromatography on a chromatotron (Harrison Research Corp.) using plates coated with silica gel 60 PF254 containing gypsum, using 5:1 hexane/EtOAc. Spectroscopic data for probe **5a** were consistent with literature data (Jones et al., 2005). ^{1}H-NMR and ^{13}C-NMR data were acquired on a Bruker Avance spectrophotometer (400 MHz for proton). ^{1}H NMR spectra were referenced internally to the residual proton resonance in $CDCl_3$ (δ = 7.26 ppm), or with tetramethylsilane (TMS, δ = 0.00 ppm) as internal standard. Chemical shifts are reported as parts per million (ppm) in the δ scale downfield from TMS. ^{13}C NMR spectra were recorded with continuous proton decoupling. Chemical shifts are reported in ppm from TMS with the solvent as the internal reference ($CDCl_3$, δ = 77.0 ppm). Accurate mass spectra were acquired using a Bruker Daltonics – ultrOTOF-Q, +ESI-Q-q-TOF.

4.6.1 Alkene probe 3b—(65%, colorless oil): ^{1}H-NMR ($CDCl_3$, 400 MHz): δ7.94 (s, 1H), 7.80 (t, 2H, *J* = 8.4 Hz), 7.53 (m, 1H), 7.15–7.23 (m, 2H), 6.57 (s, 1H), 5.47–5.66 (m, 2H), 3.94 (s, 3H), 3.13 (m, 2H), 2.05 (m, 2H), 0.98 (t, 3H, *J* = 7.6Hz). ^{13}C-NMR ($CDCl_3$, 100 MHz): δ 170.5, 159.1, 137.8, 135.5, 130.0, 128.4, 128.3, 128.0, 126.8, 125.1, 123.8, 120.1, 119.1, 116.42, 105.9. HRMS (+ESI): calculated for $C_{19}H_{19}NO_3$ $[M+Na]^+$ 332.1257, found 332.1250.

4.6.2 Epoxide probe 5b—(11%, yield yellow oil): ^{1}H-NMR ($CDCl_3$, 400 MHz): δ 8.26 (s, 1H), 7.80 (t, 2H, *J* = 8.8Hz), 7.52 (m, 1H), 7.15–7.26 (m, 2H), 6.60 (s, 1H), 3.94 (s, 3H), 3.08 (m, 1H), 2.75 (m, 1H), 2.66 (m, 2H), 1.59 (m, 2H), 0.97 (t, 3H, *J* = 5.6 Hz). ^{13}C-NMR ($CDCl_3$, 100 MHz): δ 168.8, 159.0, 135.4, 129.9, 128.2, 128.0, 127.8, 126.3, 125.0, 120.0, 116.0, 105.8, 63.4, 59.5, 55.4, 52.9, 37.3, 24.7, 9.6. HRMS (+ESI): calculated for $C_{19}H_{19}NO_4$ $[M+Na]^+$ 348.1167, found 348.1206.

4.6.3 Synthesis of *trans*-4,5-epoxy-hexanol (9), 2-methyltetrahydro-2H-pyran-3-ol (10) and 1-(tetrahydrofuran-2-yl)ethanol (11)—Syntheses were performed as previously described (Coxon et al., 1973). *Trans*-4-hexen-1-ol (500 μl, 5.88

mmol) was mixed with $NaHCO_3$ (1.775 g), acetone (5.6 ml) and EtOAc (20 ml). Oxone (2.6 g, 17.1 mmol) was dissolved in H_2O (18 ml) and added dropwise to the *trans*-4-hexen-1-ol solution over a period of 40 min. The reaction was stirred for another hour. The organic solvents were evaporated in vacuuo. The residue was extracted with EtOAc (20 ml). The organic layer was washed twice with an equal volume of brine, dried over anhydrous Na_2SO_4, filtered and the solvent evaporated *in vacuuo* to yield *trans*-4,5-epoxy-hexanol **9** which was used in the next step without further purification. Spectroscopic data for **9** were consistent with literature data. *Trans*-4,5-epoxy-hexanol **9** was treated with a solution of boron trifluoride etherate in Et_2O as described previously to produce a mixture of **10** and **11**. Analysis by GC-MS showed two products with the same *m/z* (116) in a ratio of 5:1 which were assigned as **10** and **11** respectively, based on previous reports (Coxon et al., 1973).

4.7 Cloning and expression of K. brevis EH1

Contig MGID2034061 of a *K. brevis* EST library (Lidie et al., 2005) was synthesized (after optimization of codon usage for *E. coli* expression) and cloned into pUC 57 by Genescript. The insert was subcloned into pET30a+ vector for protein expression: Specific primers (Forward: CACAATCATATGCCGCTGACGGA, Reverse: AATAAGCTTTAATGATGATGATGATGATGCAGACGGCTCTGATTTTTAT) were designed to amplify the codon optimized *K. brevis* EH. Primers incorporated HindIII (reverse primer) and NdeI (forward primer) restriction sites for directional cloning and 6 histidine codons (reverse primer). The PCR product was ligated with pET30a+ using T4 DNA ligase (Invitrogen) according to the manufacturer's instructions. The newly constructed plasmid was transformed into expression strain BL21(DE3) by electroporation. Recombinant cells were grown following manufacturer's guide (Invitrogen). White colonies were picked and grown in LB broth with kanamycin (50 μg/ml). Plasmids were extracted using QIAprep Spin Miniprep Kit (Qiagen) according to the manufacturer's instruction and sent to Eurofins Genomics for sequencing to insure fidelity of insert sequence. The recombinant *E. coli* was inoculated into LB broth with kanamycin (50 μg/ml) and shaken at 37 °C overnight. The overnight culture (5 ml) was diluted into fresh LB broth (500 ml) with kanamycin (50 μg/ml), shaken at 37 °C (250 rpm for 2 ~3 h). IPTG (1mM final concentration) was added when the OD_{600} reached to 0.6 ~0.8. After shaking another 4~6 h, the culture was centrifuged (5000 × *g* for 10 min). Lysozyme (2 μl, 50 mg/ml) and DNAse I (2 μl, 2500 unit/ml) as well as Bacterial Protein Extraction reagent (B-PER, Thermal Scientific, 4ml/ gram of cells) were added to resuspend the pellets. After incubation at room temperature for 10 min, the lysate was centrifuged (15000 × *g* for 5 min) to separate insoluble proteins. The supernatant was loaded to a column of 1 ml Ni-NTA agarose (Qiagen). The column was washed (20 mM phosphate, 0.5 M NaCl, 20 mM imidazole, 10% glycerol, pH 7.9) until no more protein was eluted (as determined by A_{280}) in the wash (typically 10 ml). This was followed by elution buffer (10 ml, 20 mM phosphate, 0.5 M NaCl, 250 mM imidazole, 10% glycerol, pH 7.9). The purified EH was dialyzed (MW cutoff 12–14 kDa) in phosphate buffer (50 mM sodium phosphate, pH 7.0) at 0°to 4°C, overnight, flash frozen in liquid N_2 and stored at −80 °C until use. Final protein concentrations ranged from 0.2 – 0.3 mg/ml.

4.8 EH assay

4.8.1 Fluorescent assay—Fluorescent probe **3a/b, 5a/b** (2 μl, 10 mM, final concentration100 μM) was added to *K. brevis* CFE (198 μl) or purified EH (198 μl) in duplicate. Fluorescence was monitored at 330 nm EX/465 nm EM (Synergy™ 2, Bioteck Instrument, Inc.) every 5 minutes at 30°C. The concentration of reporter **4** was calculated from a calibration curve prepared by measuring fluorescence of 7-methoxy-2-naphthaldehyde (0, 3.1, 12, 25, 50 μM in phosphate buffer (50 mM phosphate, pH 7.0). Fluorescence readings were normalized to protein concentration or cell number.

4.8.2 GC-MS assay—Substrate (4 mM to 10 mM final concentrations), internal standard, 1-naphthol (concentrations ranging from 0.4 to 4 mM; the concentration was optimized for each substrate to a relative response ratio of 1:5 ~5:1 for substrate/internal standard in the GC-MS), and purified EH (~0.1 mg) was combined in phosphate buffer (50 mM phosphate, pH 7.0). Aliquots were removed every 5 minutes and extracted using an equal volume of CH_2Cl_2. Samples were evaporated to dryness and reconstituted in CH_2Cl_2 to ~20 ppm. Samples were analyzed by GC-MS (Hewlett Packard 6890 with Alltech 30 m, DB5, capillary column, 0.25 mm (ID) 0.25 μm initial temperature 80 °C for 1 minute/increase to 300 °C at 10 °C/minute/hold for 7 minutes) and compared to standard curve of either the diol product or starting epoxide with the internal standard. Each reaction was performed in duplicate.

4.8.3 Cyclization reaction—*Trans*-4,5-epoxy-hexanol **9** (0.4 M stock solution in DMSO diluted to a final concentration of 4 mM) was incubated with EH1 protein (0.1 mg/ml in dialysis buffer) or dialysis buffer alone at 30°C for 1 to 3 h. The reaction was extracted using an equal volume of CH_2Cl_2. The organic extracts were evaporated to dryness and reconstituted in CH_2Cl_2 to ~20 ppm and analyzed by GC-MS as previously described.

4.9 Determination of K_m and k_{cat}

Specific enzyme activity was determined by fluorescent assay (**5a** and **5b**) or by GC-MS. EH1 protein (1.926 μM) was incubated with various substrate concentrations. For fluorescent probes (**5a**, **5b)**, the final concentrations of substrate were 0, 25, 50, 75 and 100 μM. For other substrates, the final concentrations of substrate were 4, 6, 8, and 10 mM. The assays were performed as previous described. Lineweaver-Burk plots were obtained using initial velocities of substrate and their corresponding concentration, and *Km*, *Vmax* and *Vmax/Km* were determined from the generated equation. These experiments were performed in duplicate.

4.10 Inhibition assay

IC_{50} values could be obtained by either using fixed substrate concentration with different concentration of inhibitors or with several different substrate concentrations with a fixed inhibitor concentration. IC_{50} values were determined using fluorescent substrate **5b** (100 μM). EH (0.1 mg/ml) was incubated with inhibitors for 2 min in phosphate buffer (50 mM, pH 7.0) at 30 °C prior to addition of substrate. EH activity was measure as previously described by monitoring fluorescence. Assays were performed in duplicate. By definition, the IC_{50} value is concentration of inhibitor that reduces EH activity by 50%. Six

concentrations of inhibitors (0, 2, 4, 8, 12, 16 mM) were assayed to obtain an inhibition curve of inhibition/inhibitor concentration.

4.11 Q-PCR

4.11.1 RNA isolation—*K. brevis* culture (100 ml) was centrifuged (450 × g for 5 min) at 20° C. The pellet was resuspended in H_2O (100 μl). Denaturing solution (600 μl, 5 M guanidium thiocyanate, 50 mM Tris pH 8, 25 mM sodium citrate, 0.5% w/v Sarkosyl, 2% PEG, 0.1 M DTT) were added. After standing at room temperature for 10 minutes, NaOAc (60 μl, 3 M, pH 5.2) was added and the mixture was vortexed. An equal volume of phenol: $CHCl_3$: isoamyl alcohol (125:24:1, pH 4.3), was added and the mixture centrifuged at (14,000 × g for 15 minutes at 4°C). The top (aqueous) phase was transferred to a new tube followed by addition of an equal volume $CHCl_3$: isoamyl alcohol (24:1) and the mixture was vortexed. After centrifugation (14,000 × g for 15 minutes) at 4°C, the top (aquous) phase was transferred to new tube which contains equal volume of cold EtOH. RNA was allowed to precipitate at −20 degrees overnight. The mixture was centrifuged at 4° C, for (30 minutes at 14,000 × g) and the pellet was washed with cold EtOH: H_2O (700 μl, 70:30, v/v). After air-drying, the pellet was reconstituted in H_2O (50 μl). RNA was quantitated using the Nanodrop 2000 (Thermo Scientific).

4.11.2 RT-PCR—Using the isolated RNA (~1μg) as template and oligo dT as primer (1 μl, 50 mM), cDNA was synthesized using the AMV First Strand cDNA Synthesis kit (Life Technologies) according to the manufacturer's instructions. Reverse transcriptase reactions were diluted 1:5 in H_2O. PCR reactions were carried out using the newly synthesized cDNA (1 μl of the diluted reverse transcriptase reaction), PCR mix (25 μl, iQ SYBR Green Supermix, BioRad), 1 μl of each primer (50 mM). EH primer set: forward; CAAGGTGCTGGGTCCTTTGG. Reverse; TTCCGGAGCGTTGAAACCAC. RuBisCO primers set: forward; GCAGCCTTTTATGCGGTATCG. Reverse; CACCAGCCATTCGCATCCATTT (Yoon et al., 2002). PCR reactions were monitored using the DNA Engine Opticon (MJ Research) which can detect Sybr green (excitation: 497 nm, emission: 520 nm) fluorescence. Cycling conditions: 94 °C denaturation for 1 min, annealing for 45 sec at 60°C, extension 72°C (RuBisCO primer set only, no extension time for EH primers), repeat 40 cycles. The efficiency of PCR mix was determined by titrating the template cDNA concentrations by dilution of the RT reactions (1:5, 1:25 and 1:125) in H_2O. Efficiencies were calculated to be ~90 to 95%. Threshold was set as 10 standard deviations above mean fluorescence generated during 3–15 baseline cycles.

Acknowledgments

This work was supported by the National Institute of Environmental Health Sciences (NIEHS) Grant S11 ES11181 (to K.R.); bridge funding from the FIU Division of Research and the College of Arts and Sciences (to K.R.); NIH grants 5SC1HD063059-04 and 1R15GM109254-01A1 (to F. L.) and a graduate assistantship from the FIU College of Arts and Sciences (to P.S.).

References

Altschul SF, Gish W, Miller W, Myers EW, Lipman DJ. Basic local alignment search tool. J Mol Biol. 1990; 215:403–410. [PubMed: 2231712]

Arand M, Hallberg BM, Zou J, Bergfors T, Oesch F, van der Werf MJ, de Bont JA, Jones TA, Mowbray SL. Structure of *Rhodococcus erythropolis* limonene-1, 2-epoxide hydrolase reveals a novel active site. EMBO J. 2003; 22:2583–2592. [PubMed: 12773375]

Arand M, Hemmer H, Durk H, Baratti J, Archelas A, Furstoss R, Oesch F. Cloning and molecular characterization of a soluble epoxide hydrolase from *Aspergillus niger* that is related to mammalian microsomal epoxide hydrolase. Biochem J. 1999; 344:273–280. [PubMed: 10548561]

Baldwin JE. Rules for ring closure. J Chem Soc, Chem Commun. 1976:734–736.

Barth S, Fischer M, Schmid RD, Pleiss J. Sequence and structure of epoxide hydrolases: a systematic analysis. Proteins: Struct, Funct, Bioinf. 2004; 55:846–855.

Blanc G, Agarkova I, Grimwood J, Kuo A, Brueggeman A, Dunigan DD, Gurnon J, Ladunga I, Lindquist E, Lucas S. The genome of the polar eukaryotic microalga *Coccomyxa subellipsoidea* reveals traits of cold adaptation. Genome Biol. 2012; 13:R39. [PubMed: 22630137]

Bourdelais AJ, Jacocks HM, Wright JL, Bigwarfe PM, Baden DG. A new polyether ladder compound produced by the dinoflagellate *Karenia brevis*. J Nat Prod. 2005; 68:2–6. [PubMed: 15679307]

Chou HN, Shimizu Y. Biosynthesis of brevetoxins. Evidence for the mixed origin of the backbone carbon chain and possible involvement of dicarboxylic acids. J Am Chem Soc. 1987; 109:2184–2185.

Coxon J, MPH, Swallow W. Study of hydroxyl participation in acyclic epoxide systems-acid-catalyzed rearrangements of trans-3, 4-epoxypentan-1ols, and cis-3, 4-epoxypentan-1-ols, 4, 5-epoxyhexan-1-ols, and 5, 6-epoxyheptan-1-ols. Aust J Chem. 1973; 26:2521–2526.

Demydchuk Y, Sun Y, Hong H, Staunton J, Spencer JB, Leadlay PF. Analysis of the tetronomycin gene cluster: Insights into the biosynthesis of a polyether tetronate antibiotic. ChemBioChem. 2008; 9:1136–1145. [PubMed: 18404760]

Fleming LE, Kirkpatrick B, Backer LC, Bean JA, Wanner A, Dalpra D, Tamer R, Zaias J, Cheng YS, Pierce R. Initial evaluation of the effects of aerosolized Florida red tide toxins (brevetoxins) in persons with asthma. Environ Health Perspect. 2005:650–657. [PubMed: 15866779]

Flewelling LJ, Naar JP, Abbott JP, Baden DG, Barros NB, Bossart GD, Bottein MYD, Hammond DG, Haubold EM, Heil CA. Brevetoxicosis: Red tides and marine mammal mortalities. Nature. 2005; 435:755–756. [PubMed: 15944690]

Gallimore AR, Spencer JB. Stereochemical uniformity in marine polyether ladders— implications for the biosynthesis and structure of maitotoxin. Angew Chem, Int Ed. 2006; 45:4406–4413.

Gates JA, Wilson WB. The toxicity of *Gonyaulax monilata* Howell to *Mugil cephalus*. Limnol Oceanogr. 1960; 5:171–174.

Greenbaum D, Colangelo C, Williams K, Gerstein M. Comparing protein abundance and mRNA expression levels on a genomic scale. Genome Biol. 2003; 4:117. [PubMed: 12952525]

Gruber K, Zhou B, Houk KN, Lerner RA, Shevlin CG, Wilson IA. Structural basis for antibody catalysis of a disfavored ring closure reaction. Biochemistry. 1999; 38:7062–7074. [PubMed: 10353817]

Harvey BM, Mironenko T, Sun Y, Hong H, Deng Z, Leadlay PF, Weissman KJ, Haydock SF. Insights into polyether biosynthesis from analysis of the nigericin biosynthetic gene cluster in *Streptomyces sp DSM4137*. Chem Biol. 2007; 14:703–714. [PubMed: 17584617]

Jones PD, Wolf NM, Morisseau C, Whetstone P, Hock B, Hammock BD. Fluorescent substrates for soluble epoxide hydrolase and application to inhibition studies. Anal Biochem. 2005; 343:66–75. [PubMed: 15963942]

Kim IH, Morisseau C, Watanabe T, Hammock BD. Design, synthesis, and biological activity of 1, 3-disubstituted ureas as potent inhibitors of the soluble epoxide hydrolase of increased water solubility. J Med Chem. 2004; 47:2110–2122. [PubMed: 15056008]

Lee MS, Qin G, Nakanishi K, Zagorski MG. Biosynthetic studies of brevetoxins, potent neurotoxins produced by the dinoflagellate *Gymnodinium breve*. J Am Chem Soc. 1989; 111:6234–6241.

Lee MS, Repeta DJ, Nakanishi K, Zagorski MG. Biosynthetic origins and assignments of carbon 13 NMR peaks of brevetoxin B. J Am Chem Soc. 1986; 108:7855–7856. [PubMed: 22283310]

Lidie KB, Ryan JC, Barbier M, Van Dolah FM. Gene expression in Florida red tide dinoflagellate *Karenia brevis*: analysis of an expressed sequence tag library and development of DNA microarray. Mar Biotechnol. 2005; 7:481–493. [PubMed: 15976935]

Matsuura Y, Shichijo Y, Minami A, Migita A, Oguri H, Watanabe M, Tokiwano T, Watanabe K, Oikawa H. Intriguing substrate tolerance of epoxide hydrolase Lsd19 involved in biosynthesis of the ionophore antibiotic lasalocid A. Org Lett. 2010; 12:2226–2229. [PubMed: 20394359]

Minami A, Migita A, Inada D, Hotta K, Watanabe K, Oguri H, Oikawa H. Enzymatic epoxide-opening cascades catalyzed by a pair of epoxide hydrolases in the ionophore polyether biosynthesis. Org Lett. 2011; 13:1638–1641. [PubMed: 21375229]

Minami A, Oguri H, Watanabe K, Oikawa H. Biosynthetic machinery of ionophore polyether lasalocid: enzymatic construction of polyether skeleton. Curr Opin Chem Biol. 2013; 17:555–561. [PubMed: 23796908]

Monroe EA, Van Dolah FM. The toxic dinoflagellate *Karenia brevis* encodes novel type I-like polyketide synthases containing discrete catalytic domains. Protist. 2008; 159:471–482. [PubMed: 18467171]

Morisseau C, Archelas A, Guitton C, Faucher D, Furstoss R, Baratti JC. Purification and characterization of a highly enantioselective epoxide hydrolase from *Aspergillus niger*. Eur J Biochem. 1999; 263:386–395. [PubMed: 10406946]

Morisseau C, Hammock BD. Epoxide hydrolases: mechanisms, inhibitor designs, and biological roles. Annu Rev Pharmacol Toxicol. 2005; 45:311–333. [PubMed: 15822179]

Nakanishi K. The chemistry of brevetoxins: a review. Toxicon. 1985; 23:473–479. [PubMed: 3895583]

Oliynyk M, Stark CBW, Bhatt A, Jones MA, Hughes-Thomas ZA, Wilkinson C, Oliynyk Z, Demydchuk Y, Staunton J, Leadlay PF. Analysis of the biosynthetic gene cluster for the polyether antibiotic monensin in *Streptomyces cinnamonensis* and evidence for the role of monB and monC genes in oxidative cyclization. Mol Microbiol. 2003; 49:1179–1190. [PubMed: 12940979]

Pedragosa-Moreau S, Archelas A, Furstoss R. Microbiological transformation 32: Use of epoxide hydrolase mediated biohydrolysis as a way to enantiopure epoxides and vicinal diols: Application to substituted styrene oxide derivatives. Tetrahedron. 1996a; 52:4593–4606.

Pierce RH, Henry MS. Harmful algal toxins of the Florida red tide (*Karenia brevis*): Natural chemical stressors in South Florida coastal ecosystems. Ecotoxicology. 2008; 17(7):623–631. [PubMed: 18758951]

Pleiss J, Fischer M, Peiker M, Thiele C, Schmid RD. Lipase engineering database: understanding and exploiting sequence–structure–function relationships. J Mol Catal B: Enzym. 2000; 10:491–508.

Rudberg PC, Tholander F, Andberg M, Thunnissen MM, Haeggström JZ. Leukotriene A_4 hydrolase identification of a common carboxylate recognition site for the epoxide hydrolase and aminopeptidase substrates. J Biol Chem. 2004; 279:27376–27382. [PubMed: 15078870]

Ryan DE, Pepper AE, Campbell L. De novo assembly and characterization of the transcriptome of the toxic dinoflagellate *Karenia brevis*. BMC genomics. 2014; 15:888. [PubMed: 25306556]

Shichijo Y, Migita A, Oguri H, Watanabe M, Tokiwano T, Watanabe K, Oikawa H. Epoxide hydrolase Lsd19 for polyether formation in the biosynthesis of lasalocid A: direct experimental evidence on polyene-polyepoxide hypothesis in polyether biosynthesis. J Am Chem Soc. 2008; 130:12230–12231. [PubMed: 18710235]

Smith L, Hong H, Spencer JB, Leadlay PF. Analysis of specific mutants in the lasalocid gene cluster: evidence for enzymatic catalysis of a disfavoured polyether ring closure. ChemBioChem. 2008; 9:2967–2975. [PubMed: 19025863]

Snyder R, Gibbs P, Palacios A, Abiy L, Dickey R, Lopez JV, Rein K. Polyketide synthase genes from marine dinoflagellates. Mar Biotechnol. 2003; 5:1–12. [PubMed: 12925913]

Snyder RV, Guerrero MA, Sinigalliano CD, Winshell J, Perez R, Lopez JV, Rein KS. Localization of polyketide synthase encoding genes to the toxic dinoflagellate Karenia brevis. Phytochemistry. 2005; 66:1767–1780. [PubMed: 16051286]

Sun Y, Zhou X, Dong H, Tu G, Wang M, Wang B, Deng Z. A complete gene cluster from *Streptomyces nanchangensis* NS3226 encoding biosynthesis of the polyether ionophore nanchangmycin. Chem Biol. 2003; 10:431–441. [PubMed: 12770825]

Tzeng HF, Laughlin LT, Lin S, Armstrong RN. The catalytic mechanism of microsomal epoxide hydrolase involves reversible formation and rate-limiting hydrolysis of the alkyl-enzyme intermediate. J Am Chem Soc. 1996; 118:9436–9437.

Van Dolah FM, Doucette GJ, Gulland FM, Rowles TL, Bossart GD. 10 Impacts of algal toxins on marine mammals. Toxicol Mar Mamm. 2003:247.

Vilotijevic I, Jamison TF. Epoxide-opening cascades promoted by water. Science. 2007; 317(5842): 1189–1192. [PubMed: 17761875]

Yamada T, Morisseau C, Maxwell JE, Argiriadi MA, Christianson DW, Hammock BD. Biochemical evidence for the involvement of tyrosine in epoxide activation during the catalytic cycle of epoxide hydrolase. J Biol Chem. 2000; 275:23082–23088. [PubMed: 10806198]

Yamazaki M, Izumikawa M, Tachibana K, Satake M, Itoh Y, Hashimoto M. Origins of oxygen atoms in a marine ladder-frame polyether: evidence of monooxygenation by ^{18}Olabeling and using tandem mass spectrometry. J Org Chem. 2012; 77:4902–4906. [PubMed: 22574691]

Yoon HS, Hackett JD, Bhattacharya D. A single origin of the peridinin- and fucoxanthin-containing plastids in dinoflagellates through tertiary endosymbiosis. Proc Natl Acad Sci. 2002; 99:11724–11729. [PubMed: 12172008]

Zou J, Hallberg BM, Bergfors T, Oesch F, Arand M, Mowbray SL, Jones TA. Structure of *Aspergillus niger* epoxide hydrolase at 1.8 Å resolution: implications for the structure and function of the mammalian microsomal class of epoxide hydrolases. Structure. 2000; 8:111–122. [PubMed: 10673439]

Highlights

An epoxide hydrolase (EH) from *Karenia brevis* is cloned and expressed.

Substrate selectivity of expressed EH is characterized.

High toxic *Karenia brevis* has higher EH activity when compared to a low toxic strain.

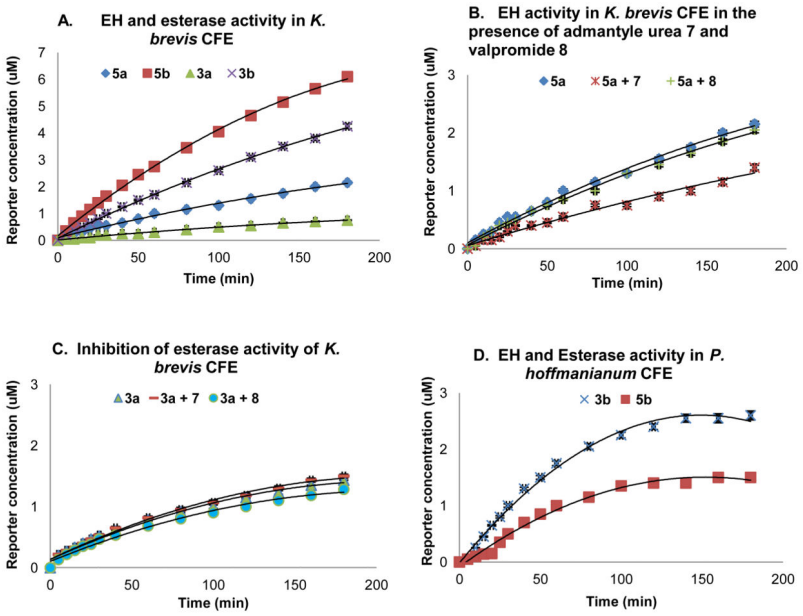

Figure 1.

EH activity in *K. brevis* and *P. hoffmanianum* CFE and sensitivity to inhibitors. A. EH (**5a**/**5b**) and esterase (**3a**/**3b**) activity. B. Inhibition of EH activity. C. Inhibition of esterase activity. D. EH (**5b**) and esterase (**3b**) activity in CFE of *P. hoffmanianum*.

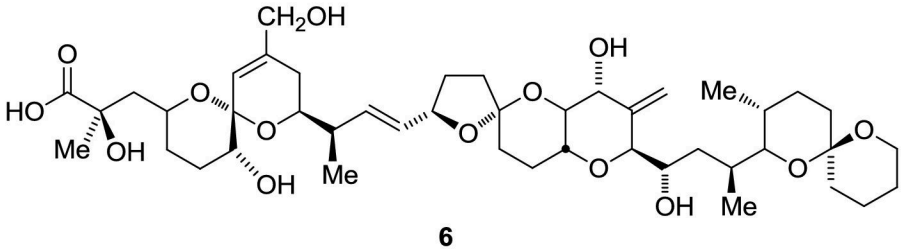

Figure 2.
Structure of okadaic acid (**6**).

A.

```
K. brevis EH    ----------MPLTDLKPFKLTVPDQQLDDLKYRISATRWPDQLDSPANANWEYGTEITYLKSLAEYWRTTFSWRKQEELLNAMPQFTAKLNGVTVHFVHQRCLSSPTAPALLICHGWPG 110
A. niger EH     MSAPFAKFPSSASISPNPFTVSIPDEQLDDLKTLVRLSKIAPPTYESLQADGRFGITSEWLTTMREKWLSEFDWRPFEARLNSFPQFTTEIEGLTIHFAALFSERE-DAVPIALLHGWPG 119
                          .  . :**.:::**:****** :  :: .    .. :*: .:*    :*.:: * * : *.**  *  **::****:::*:*:**.   .  .  * .: : *****

                                                                                                  ▼
K. brevis EH    SIFEPHKVLGPLAEN-------FHVVAPSIPGYGFSEAP-HKRGFNAPEAARLFHALMLELGY-QEYVAQGGDWGSVITQCIGKLFPKQCKAIHINMPTAPRPKD-FDMSKLNPAEVEGL 220
A. niger EH     SFVEFYPILQLFREEYTPETLFFHLVVPSLPGYTFSSGPPLDKDFGLMDNARVVDQLMKDLGFGSGYIIQGGDIGSFVGRLLGVGF-DACKAVHLNLCAMRAPPEGPSIESLSAAEKEGI 238
                *:.**: :*  : *:          **:*.**:*** **..*  .:.*.  : **:.. ** :**: . *: **** **.: : :*  * . ***:*:*: :    * :  .:..*..* **:
                             ▼                                                                    ▼                                ▼
K. brevis EH    RRTMAFNTYGTGYQKISGTKPQTLSYGLNDSPIGLLAWMTEKFRDWSDCNGTLENAFTQQELLTNAMIYWVSQSIGSSMRFYYENIAVMPGTSKEMIELAAVKVSVPTAVAMFPKEIFFC 340
A. niger EH     ARMEKFMTDGLAYAMEHSTRPSTIGHVLSSSPIALLAWIGEKYLQWVDKP------LPSETILEMVSLYWLTESFPRAIHTYRETTPTASAPNGATMLQKELYIHKPFGFSFFPKDLCPV 352
                  *   * * * .*    .*:*.*:.: *..***.****: **: :* *      :..: **  . :**::::*:  ::: * *. .. ....   :    : :  * ..::****::
                                          ▼
K. brevis EH    PRAWCEQAYNLQQYTRFEAGGHFAALEKPEELVKDIKDFFLRRLDLDKNQSRL 393
A. niger EH     PRSWIATTGNLVFFRDRAEGGHFAALERPRELKTDLTAFVEQVWQK------- 398
                **:*   : **  :  .  ********:*.** .*:. *. :  :
```

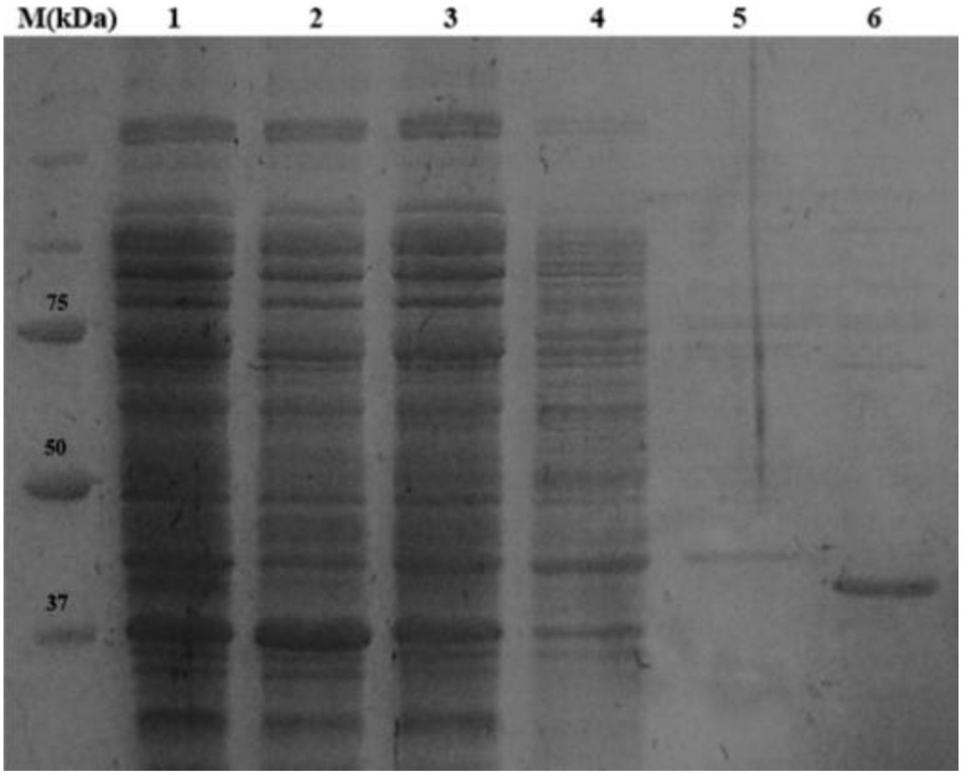

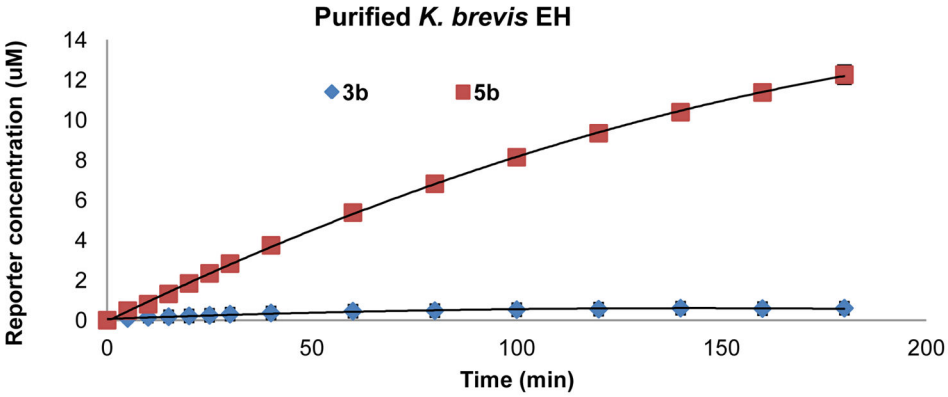

Figure 3.

A. Alignment of putative *K. brevis* EH1 with *Aspergillus niger* EH. Catalytic residues are indicated by ▼. B. SDS PAGE of expressed protein after purification and dialysis. Lanes **M**: Precision Plus Protein Unstained Standards (Biorad 161-0363) lane 1: lysate; lanes 2–3:

column flow-through; lanes 4–5: column washes; lane 6: elution. C. EH (**5b**) and esterase (**3b**) assay of purified *K. brevis* EH.

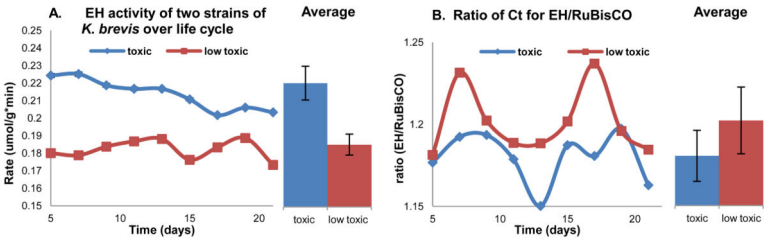

Figure 4.

A. EH activity of low and high toxin *K. brevis* CFEs over a 21 day period normalized to protein content. **B**. Ratio of C_t for EH/RuBisCO for low and high toxin *K. brevis*.

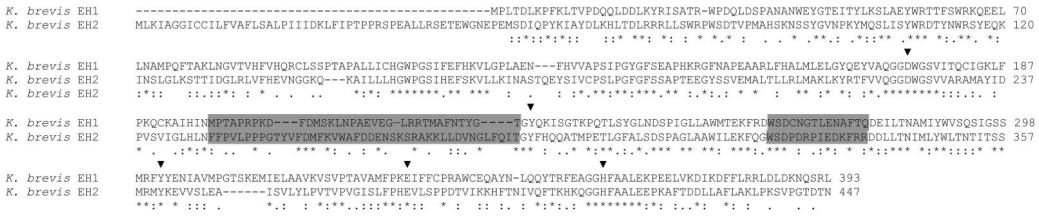

Figure 5.

Alignment of two *K. brevis* mEHs. Catalytic residues are indicated by ▼ and NC-loop and cap-loop are highlighted in grey.

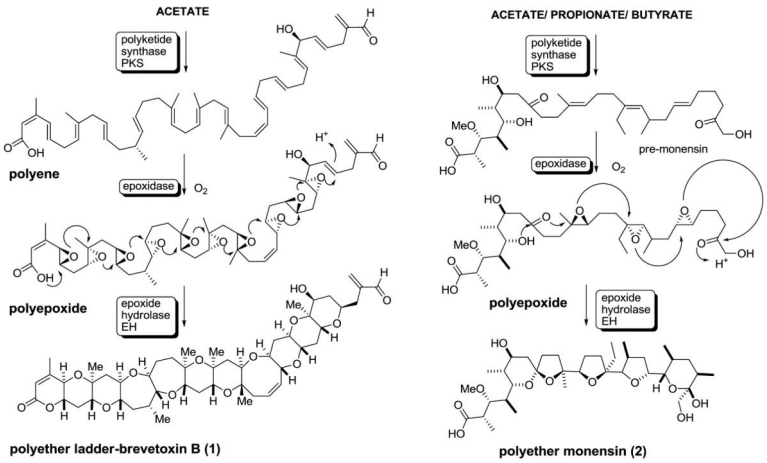

Scheme 1.

Proposed polyether ladder (left) and confirmed polyether (right) biosynthesis.

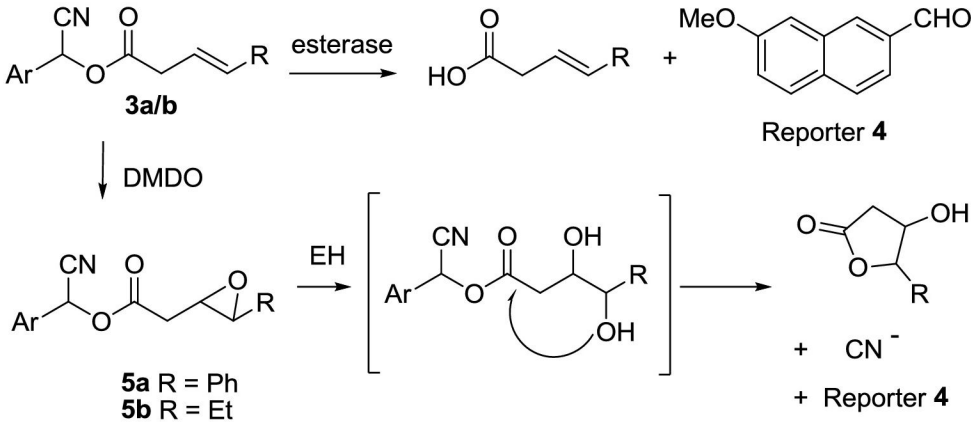

Scheme 2.

Preparation and use of EH and esterase probes.

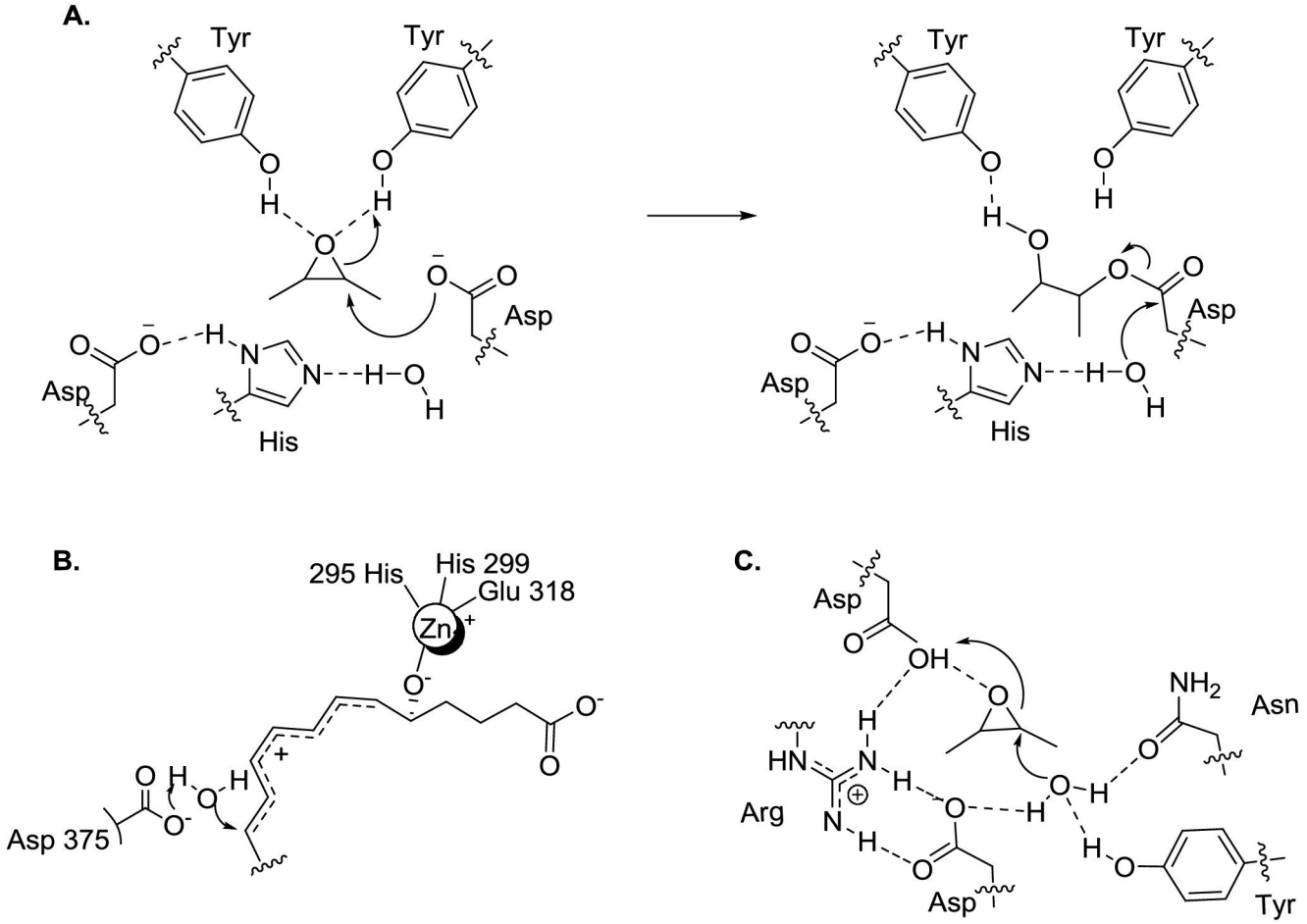

Scheme 3.

Mechanisms of epoxide hydrolases. A. The two step mechanism of the α,β-hydrolase fold type. B. leukotriene-A_4-hydrolase. C. Limonene epoxide hydrolases.

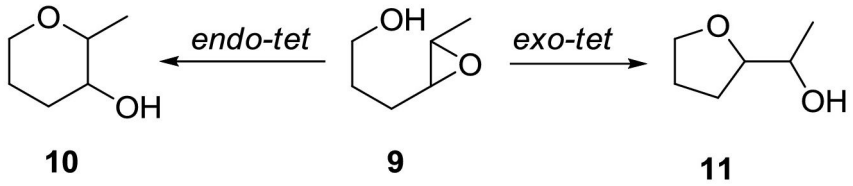

Scheme 4.

Regioisomeric cyclizations of *trans*-4,5-epoxy-hexanol (**10**).

Table 1

Kinetic parameters of the *K. brevis* EH with various substrates and inhibitors

Entry	Substrate	K_m (μM)	k_{cat} (sec^{-1})	k_{cat} (sec^{-1})/K_m (M)	IC_{50} (mM)
1	Probe **5a** (R = Ph)	13.6	7.81E-4	57.4	-
2	Probe **5b** (R = Et)	161	4.46E-3	27.7	-
3	(*R*) styrene oxide	6240	9.01E-1	144	-
4	(*S*) styrene oxide	6430	8.32E-1	129	-
5	(*R/S*) styrene oxide	6570	8.58E-1	131	-
6	α-methylstyrene oxide	5310	3.31E-1	62.3	-
7	(*R*) 1-butane oxide	25,800	6.15	238	-
8	(*R/S*) 1-butane oxide	22,200	5.36	241	-
9	1,2,7,8-diepoxyoctane	4,800	7.12	1483	-
10	*cis*-β-methylstyrene oxide	-	-	-	3.05
11	*trans*-β-methylstyrene oxide-	-	-	-	14.28
12	β-dimethylstyrene oxide	-	-	-	6.99
13	*cis*-2,3-epoxybutane	-	-	-	-
14	2,3-dimethyl-2,3-epoxybutane	-	-	-	−3